AMERICAN SOCIETY FOR MICROBIOLOGY | Antimicrobial Agents and Chemotherapy®

MECHANISMS OF RESISTANCE

Intercellular Transfer of Chromosomal Antimicrobial Resistance Genes between *Acinetobacter baumannii* Strains Mediated by Prophages

Jun-ichi Wachino,[a] Wanchun Jin,[a] Kouji Kimura,[a] Yoshichika Arakawa[a]

[a]Department of Bacteriology, Nagoya University Graduate School of Medicine, Nagoya, Aichi, Japan

ABSTRACT The spread of antimicrobial resistance genes (ARGs) among Gram-negative pathogens, including *Acinetobacter baumannii*, is primarily mediated by transferable plasmids; however, ARGs are frequently integrated into its chromosome. How ARG gets horizontally incorporated into the chromosome of *A. baumannii*, and whether it functions as a cause for further spread of ARG, remains unknown. Here, we demonstrated intercellular prophage-mediated transfer of chromosomal ARGs without direct cell-cell interaction in *A. baumannii*. We prepared ARG-harboring extracellular DNA (eDNA) components from the culture supernatant of a multidrug-resistant (MDR) *A. baumannii* NU-60 strain and exposed an antimicrobial-susceptible (AS) *A. baumannii* ATCC 17978 strain to the eDNA components. The antimicrobial-resistant (AR) *A. baumannii* ATCC 17978 derivatives appeared to acquire various ARGs, originating from dispersed loci of the MDR *A. baumannii* chromosome, along with their surrounding regions, by homologous recombination, with the ARGs including *armA* (aminoglycoside resistance), bla_{TEM-1} (β-lactam resistance), *tet*(B) (tetracycline resistance), and *gyrA*-81L (nalidixic acid resistance) genes. Notably, the eDNAs conferring antimicrobial resistance were enveloped in specific capsid proteins consisting of phage particles, thereby protecting the eDNAs from detergent and DNase treatments. The phages containing ARGs were likely released into the extracellular space from MDR *A. baumannii*, thereby transducing ARGs into AS *A. baumannii*, resulting in the acquisition of AR properties by the recipient. We concluded that the generalized transduction, in which phages were capable of carrying random pieces of *A. baumannii* genomic DNAs, enabled efficacious intercellular transfer of chromosomal ARGs between *A. baumannii* strains without direct cell-cell interaction.

KEYWORDS *Acinetobacter baumannii*, antibiotic resistance

Acinetobacter baumannii is an opportunistic Gram-negative pathogen that causes severe infections, such as ventilator-associated pneumonia and bacteremia, especially in hospitalized patients, and is frequently associated with nosocomial outbreaks (1, 2). *A. baumannii* is becoming a serious public health concern, because the pathogen has developed multidrug resistance properties against carbapenems, aminoglycosides, and fluoroquinolones, which has limited the selection of antimicrobial agents for treating *A. baumannii* infections in clinical settings (3). The worldwide spread of multidrug-resistant (MDR) *A. baumannii* is attributed to the clonal spread of specific genetic lineages, such as the international clone II (IC2) (4, 5).

Carbapenem resistance in MDR *A. baumannii* depends primarily on the production of carbapenemases, which can hydrolyze carbapenems (6, 7). One of the most common mechanisms of increased aminoglycoside resistance in MDR *A. baumannii* is the production of the 16S rRNA methyltransferase ArmA, which prevents aminoglycosides from binding to the 30S ribosomal subunit through postmodification of a specific

Citation Wachino J, Jin W, Kimura K, Arakawa Y. 2019. Intercellular transfer of chromosomal antimicrobial resistance genes between *Acinetobacter baumannii* strains mediated by prophages. Antimicrob Agents Chemother 63:e00334-19. https://doi.org/10.1128/AAC.00334-19.

Address correspondence to Jun-ichi Wachino, wachino@med.nagoya-u.ac.jp.

Received 14 February 2019
Returned for modification 20 February 2019
Accepted 22 May 2019
Accepted manuscript posted online 28 May 2019
Published 25 July 2019

residue within the aminoacyl-tRNA binding site (A site) of 16S rRNA (8, 9). These horizontally acquired antimicrobial resistance genes (ARGs) are located on plasmids and/or the chromosome of *A. baumannii*, as well as on replicons of other Gram-negative pathogens, including members of the family *Enterobacteriaceae* (10, 11).

Complete genome sequence data for several MDR *A. baumannii* clinical isolates have been deposited in databases, with the data revealing that MDR *A. baumannii* possibly harbors numerous ARGs on its chromosome rather than on plasmids, which is contrary to what is documented in the case of MDR *Enterobacteriaceae* (12–14). The naturally high competence of *A. baumannii* would accelerate the efficient uptake of ARGs through the type IV pili and the Com membrane channel, resulting in their accumulative integration into the chromosome (15–17); however, how exogenous bacterial DNA fragments carrying ARGs get transferred and integrated into other *A. baumannii* chromosomes remains largely unclear. In addition, whether and how the chromosomal ARGs act as a source for ARG transfer to other *A. baumannii* strains also remain unanswered.

Mechanisms that enable DNA transfer across bacterial cells, without cell-cell interaction, had been previously reported. Outer membrane vesicles (OMVs) associated with or including DNA represent one of the sources for delivering DNA fragments to other bacterial cells (18–21). Accordingly, ARGs, such as bla_{NDM-1} and bla_{OXA-23}, on plasmids can be transferred to *A. baumannii* by OMVs (22, 23). Moreover, the free DNA fragments released from chromosomes into the environment through cell lysis or an active machinery, such as the type IV secretion system, might serve as a means for augmented DNA transfer to other bacterial cells (24–27), with the same scenario is applicable for transducing phages and gene transfer agents (28–30). Recently, Krahn et al. demonstrated the transfer of chromosomal bla_{NDM-1} and suggested the involvement of prophages in the chromosome (14); however, involvement of prophages in transferring chromosomal ARGs to *A. baumannii* remains incompletely elucidated. Here, we assessed the phenomenon associated with the transfer of chromosomal ARGs, using *A. baumannii* strains as the model, and identified the mechanisms mediating ARG transfer. Our results provide novel insights into the mechanism involved in the transfer of chromosomal ARGs across *A. baumannii* cells in the absence of direct cell-cell interaction.

RESULTS

Transfer of ARGs without direct cell-cell interaction between *A. baumannii* strains. We used the *A. baumannii* NU-60 strain belonging to IC2 (sequence type 208) as the parent strain providing extracellular DNA (eDNA) components for our evaluation of potential ARG transfer, since it carries diverse chromosomal ARGs, including *armA* (aminoglycoside resistance), bla_{TEM-1} (β-lactam resistance), and *tet*(B) (tetracycline resistance) (Fig. 1).

We first collected the eDNA-containing components from the supernatants of 24-h liquid cultures of *A. baumannii* NU-60 by ultracentrifugation, followed by their addition to antimicrobial-susceptible (AS) *A. baumannii* ATCC 17978 and *Acinetobacter baylyi* ADP1 on agar plates. The latter two strains were used as the recipient strains for ARG transfer assays, since these have been previously prepared for various transformation assays involving acceptance of exogenous DNAs (31, 32). Subsequently, antimicrobial-resistant (AR) *A. baumannii* ATCC 17978 derivatives, with the acquired ARGs, were selected by culturing on plates containing amikacin (AMK), carbenicillin (CAR), or tetracycline (TET) (Fig. 2A). While the AMK-, CAR-, and TET-resistant derivatives were obtained on plate, no AR derivative appeared when *A. baylyi* was exposed to the eDNA-containing components. Moreover, exposure to purified DNA, extracted from bacterial cells using commercially available kits, did not produce AR derivatives on any of the plates containing the antimicrobial agents.

We next evaluated the relationship between the appearance of AR derivatives and duration of culture before collecting the supernatants (Fig. 2B). AR derivatives were obtained when we used eDNA-containing components collected from supernatants at

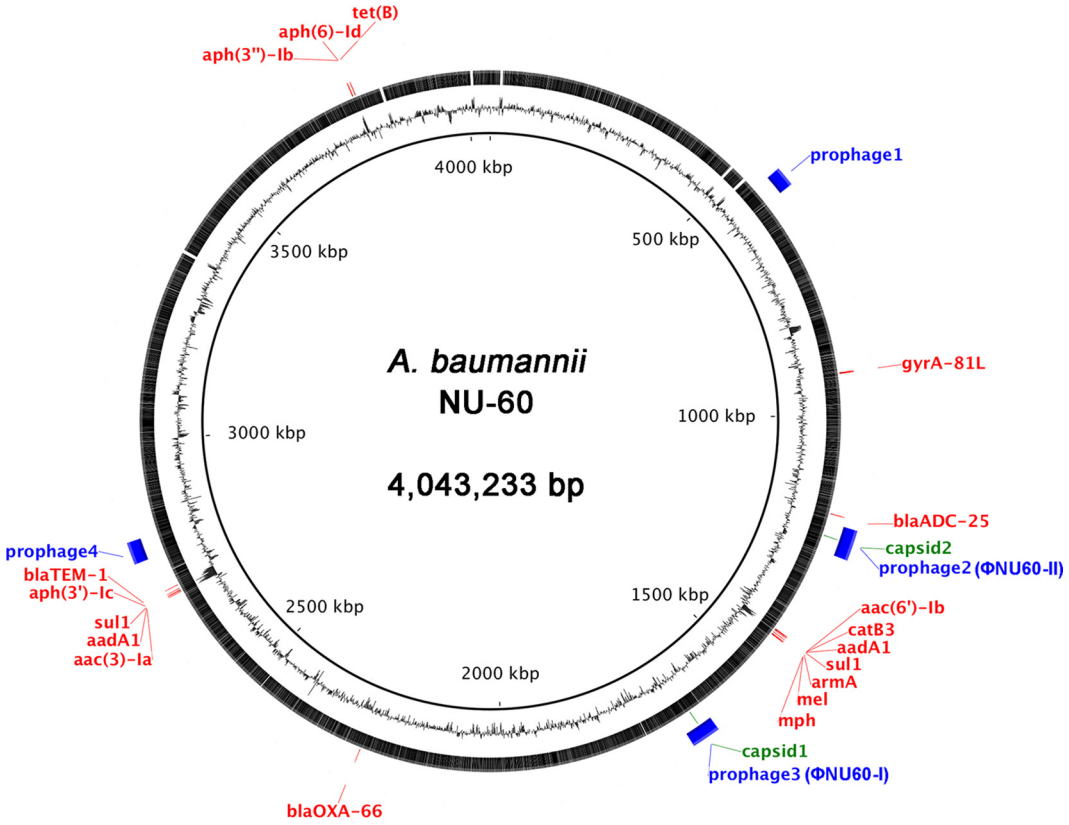

FIG 1 Circular genomic map of the *A. baumannii* NU-60 strain. The middle black line represents G+C content, followed by the *A. baumannii* NU-60 genome (black), antimicrobial resistance genes (red), capsid protein genes (green), and prophages (blue).

the exponential growth phase (6 h), with the appearance of AR derivatives increasing upon using components derived from cultures up to the stationary growth phase (24 h); however, the number of AR derivatives decreased drastically when the source cultures reached the phase of decline (48 h). The amount of eDNAs collected from supernatants changed almost in parallel with changes in the number of AR derivatives obtained and with bacterial growth (Fig. 2C); a discrepancy was observed at the 48-h time point, when larger amounts of DNA were collected, but the frequency of occurrence of AR derivatives was quite low (discussed later).

AR derivatives could acquire donor-derived ARGs and showed resistance to the corresponding antimicrobial agents. We obtained AMK-, CAR-, and TET-resistant derivatives by selecting on AMK-, CAR-, and TET-containing agar plates, respectively.

Each derivative showed resistance to the corresponding antimicrobial agent similar to that of the eDNA-providing parent *A. baumannii* NU-60 (see Fig. S1 in the supplemental material). Furthermore, we confirmed that the genes *armA*, bla_{TEM-1}, and *tet*(B) were carried by the AMK-, CAR-, and TET-resistant derivatives (ATCC 17978Ω*armA*, ATCC 17978Ωbla_{TEM-1}, and ATCC 17978Ω*tet*(B), respectively). These results together indicated that the eDNA fragments harboring the ARGs derived from the chromosome of *A. baumannii* NU-60 (Fig. 1) were released into the supernatant during liquid cultivation and that the ARGs were integrated into the recipient *A. baumannii* ATCC 17978 strain, thereby providing AR properties to the recipient.

Transfer of donor chromosomal *armA* to the recipient *A. baumannii* strain. The genetic regions surrounding *armA* in the *A. baumannii* NU-60 strain are shown in Fig. 3A. The 19-kb genetic region containing *armA* was flanked by two copies of IS*6* elements harboring 14-bp inverted repeats (IRL and IRR) at the terminal ends and showed the formation of a composite transposable element (composite transposon) known as Tn*1548* (33, 34). This composite transposon has been frequently found on the

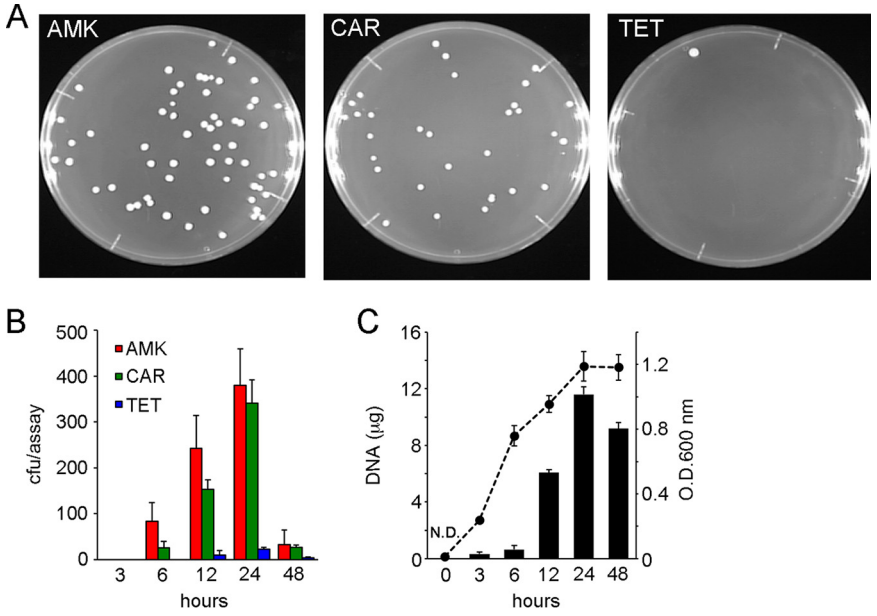

FIG 2 (A) Appearance of antimicrobial-resistant *A. baumannii* ATCC 17978 derivatives following exposure to eDNA collected from the parent *A. baumannii* NU-60 strain. AMK, amikacin; CAR, carbenicillin; TET, tetracycline. (B) Number of CFU of antimicrobial-resistant derivatives obtained after exposure to eDNA collected from culture supernatants over 48 h. The eDNA collected from 20 ml of culture supernatant at each time point was used for one assay ($n = 3$; means ± standard deviations [SD]). (C) Quantification of eDNA collected from 20 ml of culture supernatants (black bars) and optical density (O.D.) at 600 nm of bacterial cultures (black circles) ($n = 3$; means ± SD). N.D., not detected.

chromosomal/plasmid DNAs of *A. baumannii* strains isolated from geographically distinct areas (11, 35, 36). The surrounding genetic regions of Tn*1548* in the NU-60 strain were almost identical to those of the ATCC 17978 strain, indicating that Tn*1548* was horizontally inserted into the chromosome.

We determined the transferred genetic region containing *armA* in the *A. baumannii* ATCC 17978Ω*armA* strain (Fig. 3A), finding that it had captured an approximately 33-kb-long DNA fragment containing Tn*1548* of *A. baumannii* NU-60 (NU60_1322 to NU60_1286; blue-shaded region in Fig. 3A), in exchange for the original genome region (A1S_2198 to A1S_2208; 11-kb; blue-shaded region in Fig. 3A). The crossover points for the recombination were determined by aligning the *A. baumannii* NU-60, ATCC 17978Ω*armA*, and ATCC 17978 sequences. The 33-kb-long DNA fragment underwent recombination with the terminal ends at the internal positions of the genes A1S_2198 and NU60_1322 as well as A1S_2208 and NU60_1286 (Fig. 3A and Fig. S2). The ATCC 17978Ω*armA* strain likely emerged by capturing the DNA fragment of the NU-60 strain through homologous recombination, using the highly conserved genetic regions/genes in both the donor NU-60 and recipient ATCC 17978 strains.

Moreover, we investigated the transferred DNA fragment that included the *armA* gene of another amikacin-resistant derivative (*A. baumannii* ATCC 17978Ω*armA*-2), revealing that this ATCC 17978Ω*armA*-2 strain had captured an approximately 34-kb-long DNA fragment, similar to that of the *A. baumannii* ATCC 17978Ω*armA* strain; however, the nucleotide positions at which the recombination occurred was different. The right terminal end of the transposed fragment was within the A1S_2202 gene (Fig. 3A), and the left terminal end was located at the upper 12 kb of the A1S_2198 gene (not shown). The transferred genetic regions, including *armA*, differed across the investigated AMK-resistant derivatives. Nevertheless, these results showed that chromosomal *armA*, together with its long surrounding genetic regions, was transferred across *A. baumannii* without direct cell-cell interaction.

Transfer of donor chromosomal *bla*$_{TEM-1}$, *tet*(B), and *gyrA*-81L to the recipient *A. baumannii* strain. The other noninnate ARGs examined, including *bla*$_{TEM-1}$ and

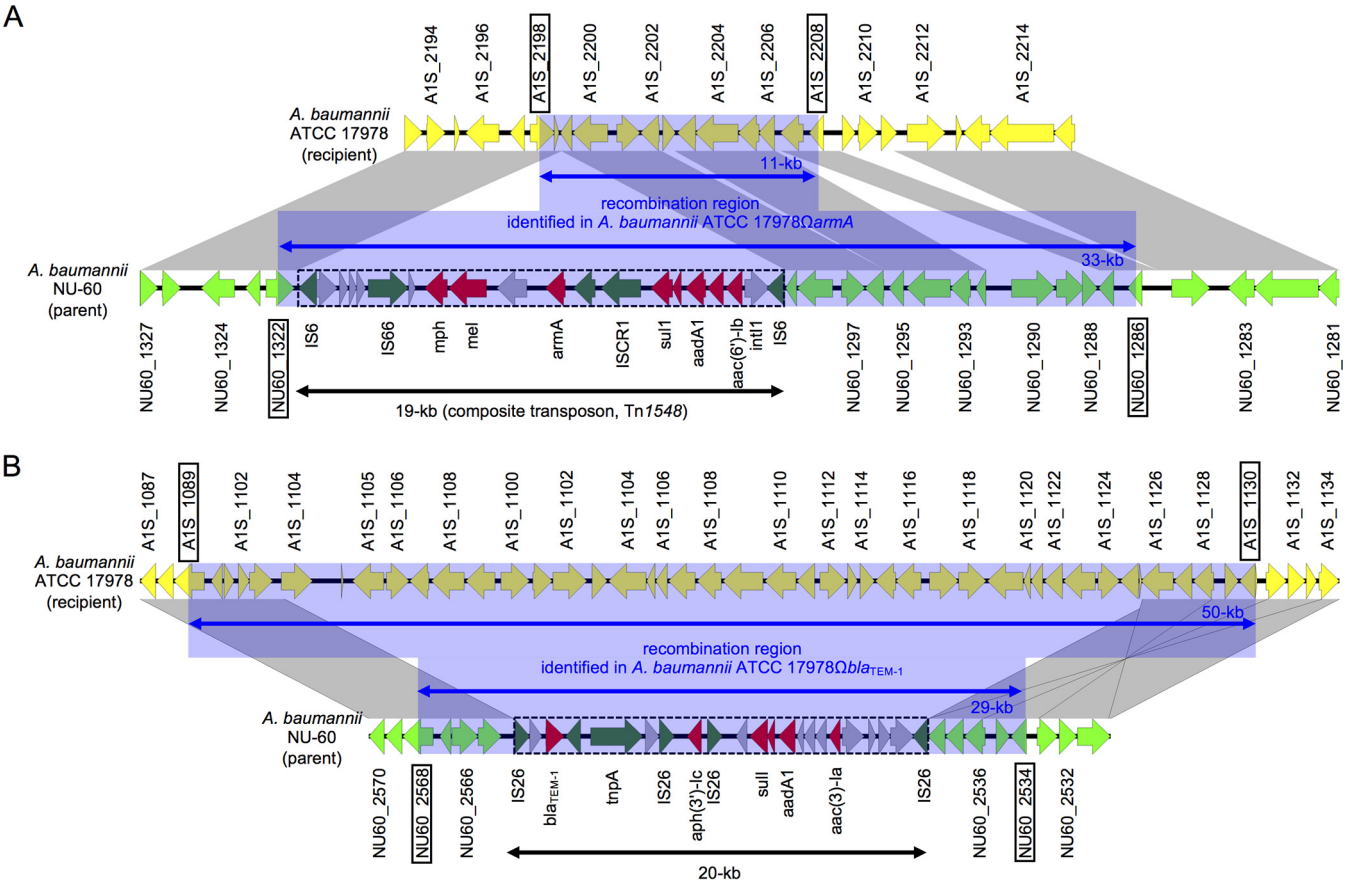

FIG 3 (A) Schematic representation of the genetic environment of 16S rRNA methyltransferase gene *armA* and its surrounding regions in *A. baumannii* NU-60 (parent). Its corresponding region of *A. baumannii* ATCC 17978 (recipient) (GenBank accession no. CP000521) is also depicted. The identified recombination regions of the *A. baumannii* ATCC 17978Ω*armA* (derivative) strain are shaded blue. Gray shades indicate the region showing genetic identity of >93%. Open reading frames (ORFs) derived from *A. baumannii* NU-60 and ATCC 17978 strains are depicted in light green and yellow, respectively. ARGs, transposase genes/insertion sequences, and hypothetical genes are shown in red, green, and gray, respectively. (B) Schematic representation of the genetic environment of bla_{TEM-1} and its surrounding regions in *A. baumannii* NU-60 (parent) and *A. baumannii* ATCC 17978 strains. The identified recombination regions of the *A. baumannii* ATCC 17978Ωbla_{TEM-1} (derivative) strain are shaded blue. Gray shades indicate the region showing genetic identity of >79%. ORFs derived from the *A. baumannii* NU-60 and ATCC 17978 strains are depicted in the same colors as those for panel A.

tet(B), were also located, similar to *armA*, on the chromosome of *A. baumannii* NU-60 (Fig. 1). We subsequently identified the genetic region containing bla_{TEM-1} that was transferred to *A. baumannii* ATCC 17978 (Fig. 3B) and found that bla_{TEM-1}, together with aminoglycoside resistance genes (*aph*, *aad*, and *aac*), was encompassed by multiple copies of IS*26*, forming a 20-kb mobile element. A 29-kb DNA fragment including bla_{TEM-1} was incorporated into the chromosome of *A. baumannii* ATCC 17978Ωbla_{TEM-1}, with recombination having occurred at the terminal ends within A1S_1089 and NU60_2568 genes (left end) and upstream of A1S_1130 and NU60_2534 (right end), resulting in the loss of a 50-kb DNA fragment. The transfer of *tet*(B) was confirmed by nucleotide sequencing of *A. baumannii* ATCC 17978Ω*tet*(B) (Fig. S3). Collectively, our analyses revealed that ARGs, which were dispersed on the chromosome of the parental NU-60 strain, were capable of being transferred to the recipient ATCC 17978 strain.

Additionally, we investigated whether chromosomal, innate, and essential genes involved in antimicrobial resistance, such as *gyrA* for quinolone resistance, were transferred through a transfer mode similar to that used for *armA*, bla_{TEM-1}, and *tet*(B). We obtained the *A. baumannii* ATCC 17978Ω*gyrA*-81L strain, showing reduced susceptibility to nalidixic acid (NA), by using the aforementioned assay. *A. baumannii* ATCC 17978Ω*gyrA*-81L emerged through the exchange of *gyrA* from *A. baumannii* ATCC 17978 (which encodes a Ser at position 81 in the quinolone resistance-determining region [QRDR]) with that of *A. baumannii* NU-60 (Leu81 in QRDR) (Table S1). The

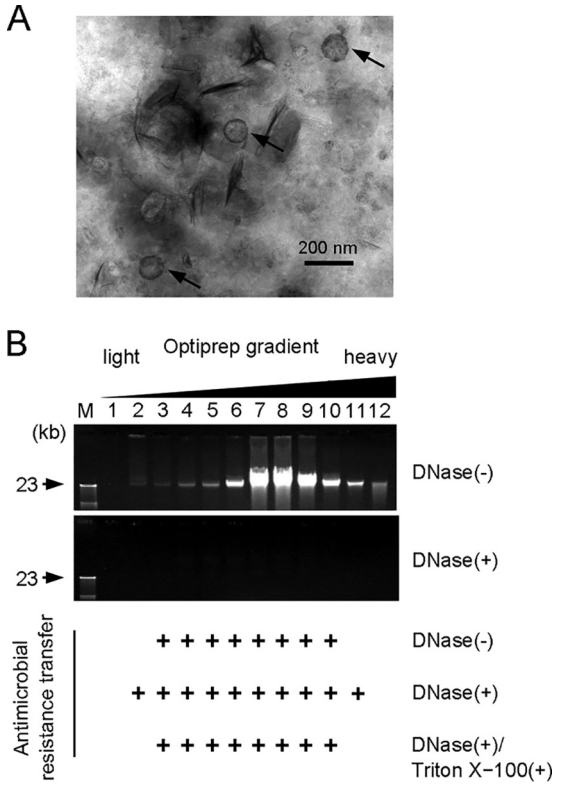

FIG 4 (A) TEM imaging of pelleted components of *A. baumannii* NU-60 culture supernatant. Bar, 200 nm. The arrows indicate OMVs. (B) Agarose gel electrophoresis of DNA-containing samples separated using an OptiPrep density gradient (10 to 45%). Samples were treated with DNase or left untreated and then electrophoresed. The samples in each fraction were treated with DNase or Triton X-100/DNase and subsequently used for the antimicrobial resistance transfer assay, which was performed three times independently. +, samples that yielded both AMK- and CAR-resistant derivatives more than twice in three trials. The result of the antimicrobial resistance transfer assay was assigned as positive upon observation of a single antimicrobial-resistant colony.

approximately 30-kb DNA fragment, including the 9.5-kb upstream and 18-kb downstream regions of *gyrA*, was exchanged through homologous recombination. These results indicated that *A. baumannii* strains successfully captured and exchanged DNA fragments, including the housekeeping genes essential for bacterial proliferation, such as *gyrA*.

Identification of eDNA used for ARG transfer. The eDNA found in culture supernatants was predicted to be present in diverse forms: naked forms released from lysed bacterial cells, OMV surface-associated forms, OMV-included forms, and phage-included forms. We performed transmission electron microscopy (TEM) analyses of the pellets containing antimicrobial resistance-conferring components, obtained after ultracentrifugation, and revealed the presence of OMVs of ~200-nm diameter (Fig. 4A). Since OMVs are capable of carrying cargo of diverse bacterial materials, including lipids, proteins, RNA, and DNA (37), we evaluated the involvement of OMV-associated/included DNA in ARG transfer. The eDNA-containing components, collected from the 24-h bacterial culture supernatant through ultracentrifugation, were subjected to density gradient ultracentrifugation using OptiPrep (10 to 45%). SDS-PAGE and Western blot analysis, performed using an antibody against the outer membrane protein A (OmpA), a primary protein component of OMVs, revealed its presence in all separated fractions (Fig. S4) (38, 39). Aliquots of the fractions obtained after ultracentrifugation were used in ARG transfer assays, revealing that exposure of *A. baumannii* ATCC 17978 to fractions 3 through 10 stably yielded AMK- and CAR-resistant *A. baumannii* ATCC 17978 derivatives (Fig. 4B). Agarose gel electrophoresis revealed the presence of condensed DNA in fractions 2 through 12 at approximately 23 kb, which probably

corresponded to the measurable DNA shown in Fig. 2C, and was susceptible to digestion by DNase; however, DNase treatment did not disturb the emergence of AMK- and CAR-resistant derivatives (Fig. 4B). Since DNase can access both naked DNA and OMV surface-associated DNA, the obtained DNA that was readily digested by DNase was unlikely to be used for the ARG transfer phenomenon observed in this study. Triton X-100 treatment is capable of lysing OMVs (40, 41), resulting in the leakage or release of DNA contained within OMVs; previous studies had shown Triton X-100 treatment prevents the transfer of ARG-carrying plasmids, wrapped within OMVs, to AS *A. baumannii* cells (22, 23). In the present study, Triton X-100/DNase double treatment failed to interrupt the emergence of AR derivatives (Fig. 4B), suggesting that OMV-containing DNA does not primarily contribute to the ARG transfer observed under the experimental conditions employed in this study.

Involvement of prophage-encoded capsid proteins in the transfer of chromosomal ARGs. TEM examination of OptiPrep-separated fractions revealed the predominant presence of OMVs in each fraction, in addition to small amounts of phage-like particles, including long tails either with or without phage head-like components (Fig. S5). We hypothesized that these components can internally store ARG-carrying DNA of the host bacterial strain and deliver it to other bacterial cells. To verify this hypothesis, we purified the OptiPrep-fractionated samples using size exclusion chromatography. Fractions 8 through 10, obtained after OptiPrep gradient ultracentrifugation (Fig. 4B), which stably generated AMK- and CAR-resistant derivatives and included only small amounts of OMV-derived components (Fig. S4), were collected and subjected to size exclusion chromatography. We observed two major peaks (Fig. 5A), and AR derivatives emerged when the fractions associated with the first peak were used in the ARG transfer assay. TEM examination of the components in the fractions (Fig. 5A, fractions a, b, and c) revealed the presence of phage particles featuring a hexagonal head (15 to 60 nm) with or without a long tail (200 to 250 nm), as well as the presence of small OMVs (30 to 50 nm) (Fig. 5B). Notably, the OMVs were lysed upon Triton X-100 treatment, whereas the phage head-like particles with long tails retained their original shapes after detergent treatment (Fig. 5B). Moreover, the emergence of AMK-, CAR-, and TET-resistant derivatives occurred when the three fractions (Fig. 5A, fractions a, b, and c) were used in the ARG transfer assay after treatment with Triton X-100. These results indicated that Triton X-100-tolerant phage particles represented a candidate agent mediating the ARG transfer.

To identify the proteins associated with the phage particles, we performed SDS-PAGE using the three fractions (Fig. 5A, fractions a, b, and c). Three major bands (identifiers [IDs] 01, 02, and 03), commonly observed in all three fractions (Fig. 5C), were subjected to nano-liquid chromatography-tandem mass spectrometry (LC-MS/MS) analysis, followed by Mascot database searches, in order to identify the composition of the proteins (Fig. 5D). Two of them (IDs 01 and 03) were predicted to be uncharacterized (hypothetical) proteins, whereas the third one (ID 02) was identified as a capsid protein. Therefore, we predicted that oligomerized capsid proteins could carry, as internal cargo, DNA fragments, including ARGs of the host *A. baumannii* strain, and that the presence of capsid proteins could contribute to diminishing the susceptibility of DNA to Triton X-100/DNase treatment. *A. baumannii* NU-60 harbored the genes for two highly similar capsid proteins, here named capsid 1 (detected using nano-LC-MS/MS and Mascot analyses) and capsid 2 (Fig. 1 and Fig. S6). To evaluate the role of these capsid proteins in ARG transfer, we constructed three deletion mutants of the capsid protein genes (Δ*capsid1*, Δ*capsid2*, and Δ*capsid1*-Δ*capsid2* mutants) in the parent NU-60 strain and measured the efficiency of ARG transfer (Fig. 6A). AMK- and CAR-resistant derivatives were generated with 20- and >40-fold lower efficiencies, respectively, when we used ultracentrifuged components from the Δ*capsid1* mutant strain supernatant than when we used the corresponding components from the NU-60 parent strain. Conversely, deletion of the capsid 2 gene did not substantially alter ARG transfer efficiency; however, deletion of both capsid 1 and 2 genes attenuated the emergence of AR derivatives (i.e., the emergence was below the detection limit of the

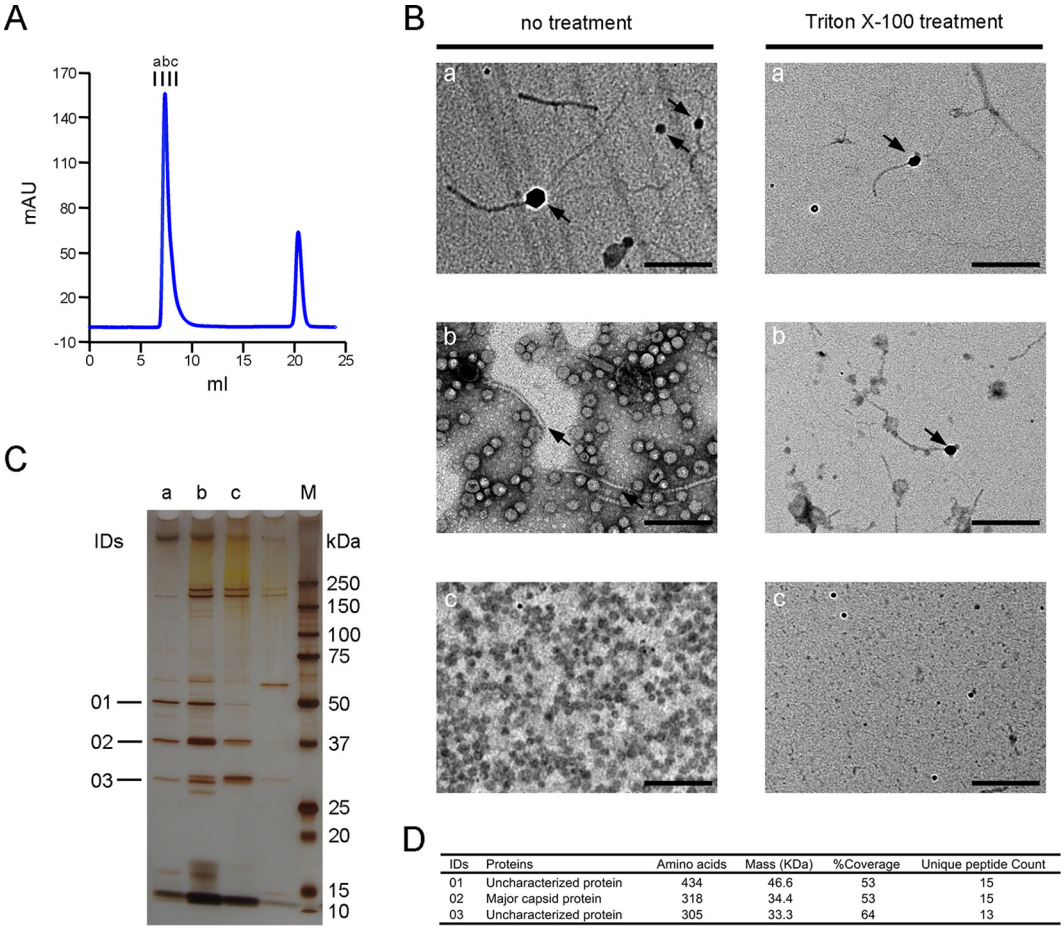

IDs	Proteins	Amino acids	Mass (KDa)	%Coverage	Unique peptide Count
01	Uncharacterized protein	434	46.6	53	15
02	Major capsid protein	318	34.4	53	15
03	Uncharacterized protein	305	33.3	64	13

FIG 5 (A) Size exclusion chromatography. AU, arbitrary units. (B) TEM imaging of fractions (a to c) separated by size exclusion chromatography as shown in panel A. Arrows indicate fraction components other than OMVs, including phage particles with or without long tails. The samples in each fraction were treated with Triton X-100 or left untreated. (C) SDS-PAGE and silver staining of samples (fractions a to c). Lane M, protein size marker. (D) Summary table of Mascot identification of proteins assigned IDs 01 to 03 in panel C.

assay). These results indicated that capsid 1 is critically involved in enabling ARG transfer and that capsid 2 moderately promotes transfer. When providing ultracentrifuged components of the NU-60 parent strain treated with mitomycin C, increased efficiency of ARG transfer was observed in a dose-dependent manner, implying that excessive phages, induced via mitomycin C treatment, relatively enhanced the chances of transducing ARGs (Fig. 6B).

To identify prophages hidden in the chromosomal DNA of the NU-60 strain and encoding capsid 1 and 2 proteins, we used the PHAge Search Tool Enhanced Release (PHASTER) server. Analyses revealed the presence of four intact prophages in the chromosome, with the capsid 1 and 2 genes associated with prophage ϕNU60-I (50.0 kb) and ϕNU60-II (52.6 kb), respectively (Fig. 1 and Fig. S7). The genes coding for two of the proteins (IDs 01 and 03) (Fig. 5D) identified by LC-MS/MS analysis were located outside the prophage regions predicted by the PHASTER server; the role of these proteins remains unclear in this study.

Generalized transduction mediates chromosomal ARG transfer. Illumina short reads prepared from the samples related to phage particles (sample 1, fractions 3 to 10 collected after OptiPrep gradient ultracentrifugation with Triton X-100/DNase treatment [Fig. 4B]; sample 2, fraction a obtained after size exclusion chromatography with Triton X-100/DNase treatment [Fig. 5A]) were mapped to the genome of the NU-60 strain (Fig. 1). The output reads derived from DNA included in the phage particles

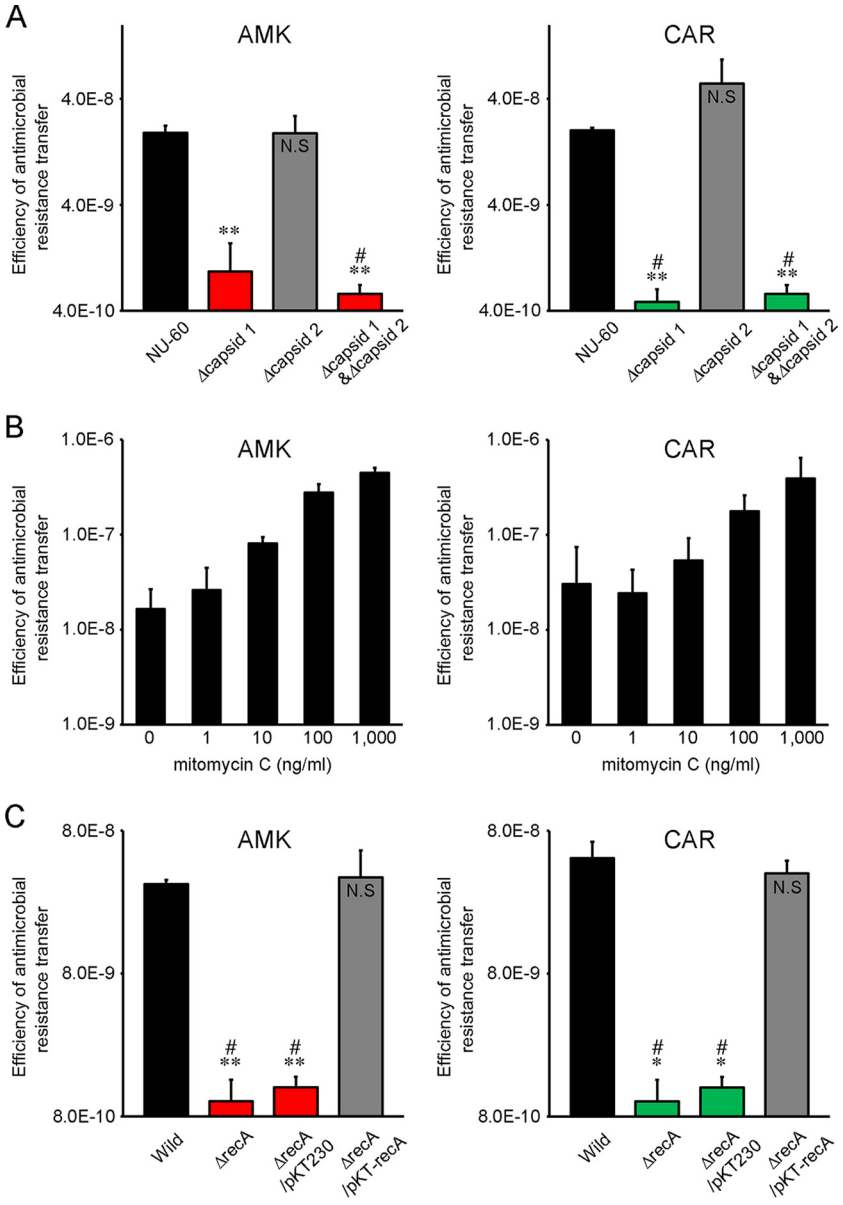

FIG 6 (A) Antimicrobial resistance transfer efficiencies calculated by counting colonies selected on AMK and CAR plates. Bars, means ± SD ($n = 3$). A sample corresponding to the supernatant of a 1.65-ml bacterial culture of *A. baumannii* NU-60 and Δ*capsid1*, Δ*capsid2*, and Δ*capsid1*-Δ*capsid2* mutants was used for each antimicrobial resistance transfer assay. Statistical significance was determined by Welch's *t* test relative to results obtained for the NU-60 strain. **, $P < 0.01$; #, limit of detection (no colony growth on plates containing antimicrobials); N.S., not significant. (B) Trend of antimicrobial resistance transfer efficiencies under mitomycin C treatment. A sample corresponding to the supernatant of an 8.25-ml culture of *A. baumannii* NU-60 was used for each antimicrobial resistance transfer assay. Bars, means ± SD ($n = 3$). (C) Antimicrobial resistance transfer efficiencies when *A. baumannii* ATCC 17978 (wild) and Δ*recA*, Δ*recA*/pKT230, and Δ*recA*/pKT230-*recA* mutants were used as the recipient cells. Bars, means ± SD ($n = 3$). A sample corresponding to the supernatant of a 5.5-ml bacterial culture of *A. baumannii* NU-60 was used for each antimicrobial resistance transfer assay. Statistical significance was determined by Welch's *t* test relative to results obtained for the wild strain. **, $P < 0.01$; *, $P < 0.05$; #, limit of detection (no colony growth on plates containing antimicrobials); N.S., not significant.

covered 44% (sample 1) and 37% (sample 2) of the length of the *A. baumannii* NU-60 genome (4,043,233 bp). These results suggested that the phage particles were capable of carrying random pieces of the host *A. baumannii* genome, except phage DNA, for assembly.

The results of quantitative PCR (qPCR) analyses for estimating the copy numbers of the capsid genes and ARGs (*armA* and bla_{TEM-1}) in the phages indicated that most of the

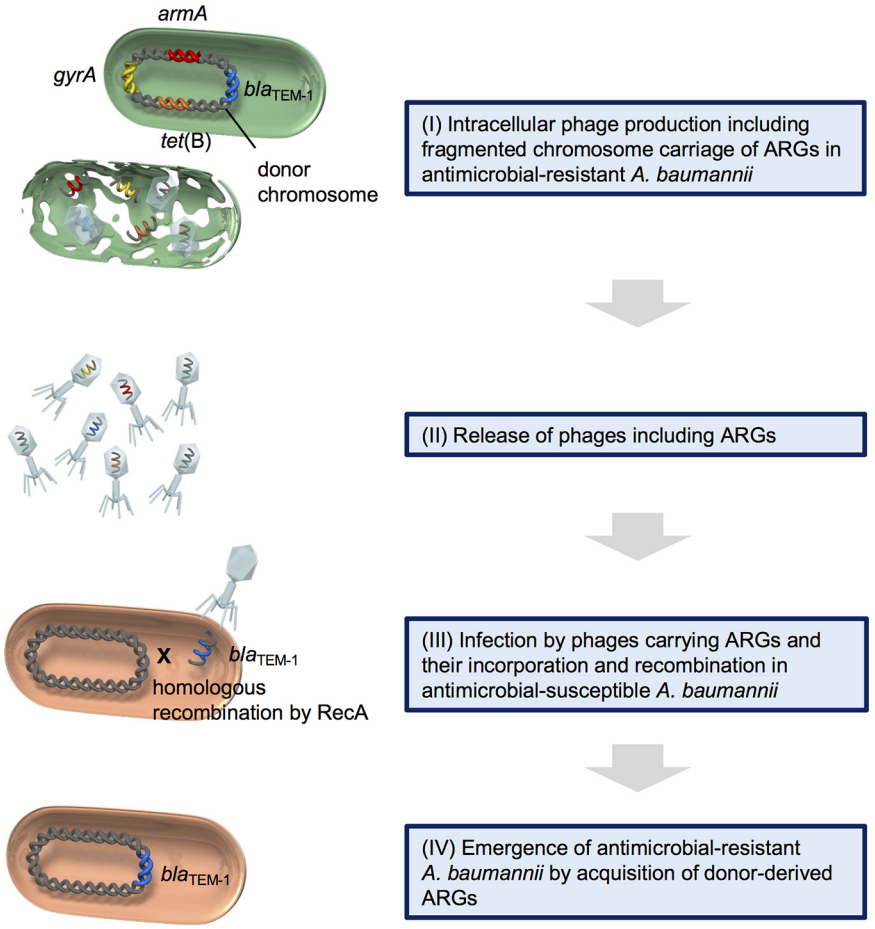

FIG 7 Summary model of ARG transfer between *A. baumannii* via generalized transduction.

phage cargo was comprised of portions of the genome required for assembling particles, such as capsid proteins, rather than non-phage-related genes, including ARGs, since the copy number of capsid 1 genes was approximately 10^3- to 10^4-fold larger than that of *armA* and bla_{TEM-1} (Fig. S8).

Finally, we evaluated whether *recA*, which generally mediates homologous recombination events in bacterial cells, contributes to the acquisition of ARG-containing fragments conveyed by phages in the recipient *A. baumannii* strain. Disruption of *recA* avoided the emergence of AMK- and CAR-resistant derivatives completely, while complementation of *recA* successfully recovered the ability to acquire ARGs (Fig. 6C). These results together indicated that *recA* plays a central role in acquiring ARGs, conveyed by phages, through homologous recombination in the recipient *A. baumannii* cells.

Collectively, our results demonstrated that ARG transfer occurred due to the generalized transduction mechanism triggered by prophages hidden in the *A. baumannii* genome. In the majority of the produced phages, DNAs for their assembly are enveloped, whereas such phages occasionally mispack host bacterium-derived genomic DNA, including ARGs. Here, the mispacked DNA, including the ARGs in the phages, were used to transfer AR properties to the AS *A. baumannii* strains, resulting in emergence of new AR organisms (Fig. 7).

DISCUSSION

Horizontal transfer of ARGs in *A. baumannii* is recognized as being primarily mediated by plasmids. However, plasmid transfer representatively mediated by conjugation presents several limitations, such as the requirement for direct cell-cell interaction, which might unexpectedly trigger cell-cell killing through type VI secretion systems (42,

43). Therefore, bacteria might benefit by transferring ARGs without direct cell-cell interaction in order to avoid disadvantages associated with such interaction. Here, we elucidated the mechanism mediating this DNA transfer, in the absence of direct cell-cell interaction, to establish the transfer of chromosomal ARGs between *A. baumannii* strains.

Consequently, a small portion of phage-related DNA in culture supernatant was employed as the cause of ARG transfer. Since the involvement of prophages in gene transfer is well known in the ordinal bacterial community as generalized transduction, it was expected to be involved in the spread of ARG across recent clinically relevant pathogens. However, the evidence explaining its contribution to the ARG transfer phenomenon in recent clinically relevant Gram-negative pathogens, including *A. baumannii*, has not yet been revealed, despite such pathogenic bacteria having rapidly acquired a variety of ARGs and generalized transduction being identified as the principal mechanism for ARG transfer in the clinically relevant Gram-positive pathogen *Staphylococcus aureus* (44).

Here, we revealed that specific prophages hidden in the chromosome of MDR *A. baumannii* could mediate the transfer of a variety of chromosomal ARGs. ARG transfer was found to be mediated by a generalized transduction mechanism in which shared DNA (including the ARGs) possibly was packed in phage particles comprised of specific capsid proteins, was discharged along with the phages following phage-related lysis, and got transferred to the recipient *A. baumannii* strains (Fig. 7). DNA fragments transferred to the recipient cells then may be integrated into the corresponding regions of the chromosome through RecA-dependent homologous recombination (Fig. 7). This type of ARG transfer, ultimately completed through homologous recombination, is in line with the finding that ARG transfer occurred with other *A. baumannii* cells but not with *A. baylyi* cells, despite the latter exhibiting an alternative yet highly competent nature.

The transferred genetic regions, including ARGs, were all consistently around 30 kb in size, despite the DNA fragments including diverse ARGs. Therefore, we expected that the phages would also contain DNA of approximately aligned sizes, which is in agreement with the characteristics of typical transducing phages enveloping regular-sized DNA (45).

Our findings are in agreement with the previous report by Krahn et al., which showed horizontal transfer of chromosomal ARGs in *A. baumannii* strain R2090 (14); it demonstrated the transfer of bla_{NDM-1} along with its 66-kb surrounding region located on the chromosome between *A. baumannii* strains and further suggested that prophage genomes located on the chromosome contributed to the transfer. The ϕR2090-I prophage region was similar to that of the ϕNU60-I prophage in the present study; proteins encoded by 25 of the 58 predicted genes of ϕNU60-I were identified in the ϕR2090-I prophage with at least 90% amino acid identities. Although the contribution of ϕR2090-I prophage to ARG transfer was not completely revealed, it was assumed to be involved in the bla_{NDM-1} transfer. These findings suggested that prophages indeed play a crucial role in transferring chromosomal ARGs, along with long surrounding DNA regions, in *A. baumannii*.

Phages carrying ARGs have been identified in diverse environments, such as in urban wastewater, environmental water, and human fecal samples (46–49), and horizontal gene transfer of ARGs through phage transduction is regarded as a cause for the emergence and spread of AR bacteria in the environment. Our results showed that DNA packed in phages tolerated nuclease and detergent treatments and that this property might enable ARG retention for an extended period in various environments, thereby augmenting opportunities for their acceptance by other bacteria. Considering the advantage offered by the protection of ARGs in phage particles, phages could be expected to play a central role in spreading ARGs in the environment without direct cell-to-cell interaction. Therefore, ARG-carrying phage particles, produced by MDR bacteria such as *A. baumannii* in clinical settings, might represent a principal vehicle for ARG dissemination across the microbial environment. Our *in vitro* model for phage-

mediated ARG transfer supports the concept of ubiquitous ARG circulation in the environment.

We used one representative *A. baumannii* clinical isolate to evaluate the phage-mediated intercellular transfer of chromosomal ARGs. Although the presence of an identical ϕNU60-I prophage (50 kb), carrying the capsid 1 gene found in the NU-60 genome, has not been admitted in any *A. baumannii* genome deposited in the database, the core capsid 1 protein gene involved in ARG transfer has been widely presented in *A. baumannii* strains isolated from geographically different areas, such as Japan (50), South Korea (51), China (52), Malaysia (53), and the United Kingdom (54). A similar phenomenon concerning the transfer of ARGs, using pelleted particles obtained through ultracentrifugation of culture supernatants, was identified when we used other *A. baumannii* clinical isolates (data not shown). However, a definitive correlation between the presence of capsid protein genes identified in this study and the phenomenon of ARG transfer was not observed. In certain strains harboring the capsid protein genes ARG transfer has not been demonstrated, whereas in other strains lacking the capsid protein genes ARG transfer did occur. Therefore, ARG transfer might be mediated by a variety of prophages hidden in the chromosome of a host *A. baumannii* strain. The extent to which these mechanisms are applicable for eDNA transfer might differ in each *A. baumannii* strain, potentially resulting in diverse eDNA transfer abilities. Future studies for investigating the relationship between capsid protein genes in prophages and ARG transfer phenomena, using other *A. baumannii* isolates, will address this question.

In conclusion, we described the efficacious phage-mediated horizontal transfer of chromosomal ARGs across *A. baumannii* strains. *A. baumannii* can release various forms of eDNA, some of which are readily degraded by DNase while others are protected from DNase digestion. In this study, we observed that DNA protected from DNase digestion by phages was transferred across *A. baumannii* strains (Fig. 7). Additionally, horizontal gene transfer is a major driving factor in the spread of ARGs among pathogenic bacteria, and our findings suggested that phages contribute to this phenomenon, likely in environments where direct cell-to-cell interaction occurs infrequently. Our study provides novel insights into the horizontal transfer of recent ARGs in the human opportunistic pathogen *A. baumannii*, with this finding offering a better understanding of *A. baumannii* evolution in terms of acquisition of MDR.

MATERIALS AND METHODS

Bacterial strains. *A. baumannii* and *A. baylyi* strains used in this study were routinely cultured in Luria-Bertani (LB) broth, supplemented with appropriate antimicrobials or left unsupplemented, at 37°C.

NGS analyses. DNA used for next-generation sequencing (NGS) analyses was extracted using a QIAamp DNA minikit (Qiagen, Hilden, Germany). To determine the complete genome sequence of *A. baumannii* strain NU-60, DNA was subjected to a PacBio RS2 sequencer with P6C4 chemistry (PacBio, Menlo Park, CA, USA). *De novo* assembly of the obtained reads (average length, 11 kb) was performed using Canu (55). Error correction of the assembled circular sequence was performed using Pilon (56) with Illumina short reads, which were obtained with a Nextera XT DNA library kit (Illumina, San Diego, CA, USA), MiSeq reagent kit, version 3 (600 cycles; Illumina), and a MiSeq platform (Illumina). Annotation was performed using the DFAST server (57).

Whole-genome sequencing analyses of *A. baumannii* ATCC 17978Ω*armA*, Ωbla_{TEM-1}, Ω*tet*(B), and Ω*gyrA*-81L derivatives were performed using Illumina short reads and an assembler of the A5-miseq pipeline (58). Gap closing was performed with classical PCR and Sanger sequencing analyses. Illumina short reads were also mapped to the *A. baumannii* NU-60 genome sequence using CLC Genomic Workbench (Qiagen) with default parameters. The ResFinder (59) and PHASTER (60) servers were used to detect ARGs and prophages in the genome of *A. baumannii*. A circular genomic map of the *A. baumannii* NU-60 strain was rendered using BLAST Ring Image Generator (BRIG) (61).

PCR detection of ARGs. Conventional PCR detection of *armA*, bla_{TEM-1}, and *tet*(B) in *A. baumannii* strains was performed using the primers listed in Table S2 in the supplemental material. The amplified products of *armA*, bla_{TEM-1}, and *tet*(B) were 315 bp, 824 bp, and 264 bp, respectively.

Introduction of ARGs into *A. baumannii*. The *A. baumannii* strains used for ARG transfer were precultured in LB broth containing 25 μg/ml AMK, and aliquots of the cultures were inoculated into plain LB broth, followed by incubation at 37°C with shaking (120 rpm). Mitomycin C was added to a final concentration of 1, 10, 100, and 1,000 ng/ml, when necessary. The bacterial cells were removed by centrifugation at 6,000 $\times$ *g* for 15 min, and the supernatant was passed through a 0.22-μm polyvinylidene difluoride (PVDF) filter (Sartorius, Göttingen, Germany). The filtrate was ultracentrifuged at

150,000 × *g* for 90 min at 10°C in a Type 50.2 Ti rotor (Beckman Coulter, Brea, CA, USA) to pellet the particles in the supernatant. The pelleted particles were resuspended in 20 mM HEPES-NaOH buffer (pH 7.5) and passed through a 0.22-μm PVDF filter. An aliquot of each sample was spread on LB-agar plates to check for donor cell (*A. baumannii* NU-60 strain) contamination in the samples; it was confirmed that there was no contamination in any prepared sample.

A. baumannii strain ATCC 17978 was cultured in LB broth at 37°C with shaking until the optical density at 600 nm reached 0.5, after which 1 ml of the bacterial culture was pelleted by centrifugation, and cell pellets were resuspended in 50 μl of phosphate-buffered saline and spotted on LB-agar plates. After air drying the surface of the spotted bacterial suspensions, the samples collected by ultracentrifugation of culture supernatants were overlaid on the dried bacterial spots, and the plates were incubated at 30°C for 24 h. The bacterial cells that grew on the LB-agar plates were scraped into 1 ml of LB broth and suspended with vigorous shaking. Finally, 100 μl of the bacterial suspension was spread on LB-agar plates supplemented with AMK (25 μg/ml), TET (50 μg/ml), CAR (400 μg/ml), or NA (75 μg/ml), and the AR derivatives assumed to have acquired antimicrobial resistance were selected.

Antimicrobial susceptibility testing. Antimicrobial susceptibility was tested according to the method provided by Clinical and Laboratory Standards Institute (62). Bacterial suspensions were adjusted to 10^8 CFU/ml in Mueller-Hinton (MH) broth (Becton, Dickinson, Franklin Lakes, NJ, USA) and spread on MH-agar plates using a sterile cotton swab, followed by placement of an Etest strip (bioMérieux, Marcy-l'Étoile, France) on the plates and incubation at 35°C for 18 h.

DNA visualization and quantification. DNA was visualized using agarose gel electrophoresis and ethidium bromide staining and quantified using a Qubit dsDNA HS assay kit and a Qubit 4 fluorometer (Thermo Fisher Scientific, Waltham, MA, USA).

TEM analysis. Samples were pipetted onto Parafilm, and TEM grids were layered on the samples. After incubation for 3 min at room temperature, the grids were layered on drops of uranyl acetate solution. The samples were viewed using a JEM-1400EX transmission electron microscope (JEOL, Tokyo, Japan).

Purification of DNA involved in ARG transfer. The precipitated particles collected after ultracentrifugation of bacterial culture supernatants were suspended in 20 mM HEPES buffer (pH 7.5) containing 45% (vol/vol) OptiPrep (Axis-Shields, Dundee, Scotland). The samples were placed at the bottom of ultracentrifugation tubes, layered with 35%, 30%, 25%, 20%, 15%, and 10% OptiPrep solution separately, and ultracentrifuged at 100,000 × *g* for 16 h at 10°C in an SW41 Ti rotor (Beckman Coulter). An aliquot was collected from the top of the supernatant and used for the ARG transfer experiment. The separated samples were treated with DNase I (TaKaRa, Shiga, Japan) and/or Triton X-100 (Sigma-Aldrich, St. Louis, MO, USA) as required.

Samples obtained after OptiPrep gradient ultracentrifugation were buffer exchanged into 20 mM HEPES-NaOH (pH 7.5) containing 100 mM NaCl using Amicon Ultra-15 filter units (Millipore, Billerica, MA, USA). The samples were loaded onto a Superdex 200 Increase 10/300 GL column (GE Healthcare, Little Chalfont, UK) and eluted with 20 mM HEPES-NaOH (pH 7.5) containing 100 mM NaCl.

SDS-PAGE and Western blotting. Samples were separated using SDS-PAGE and stained using Coomassie brilliant blue (Nacalai Tesque, Kyoto, Japan) or a Sliver Stain MS kit (FUJIFILM Wako Pure Chemical Corporation, Osaka, Japan). The separated proteins were transferred to nitrocellulose membranes, and the protein band corresponding to OmpA was detected using rabbit anti-OmpA primary antiserum (1:1,000; Eurofins Genomics, Tokyo, Japan), a horseradish peroxidase-conjugated secondary antibody (goat anti-rabbit IgG; 1:1,000; Medical & Biological Laboratories, Nagoya, Japan), and Immuno-Star Zeta (FUJIFILM Wako Pure Chemical Corporation). Protein bands were imaged using an Amersham Imager 600 system (GE Healthcare).

Identification of phage-associated proteins. Silver-stained protein bands on SDS-PAGE gels were excised, trypsin digested, and subjected to nano-LC-MS/MS and Mascot search analyses by Japan Bio Services Co., Ltd. (Saitama, Japan).

Deletion and replacement of genes in *A. baumannii*. Capsid genes were deleted in *A. baumannii* strain NU-60 according to a previous method (63). Briefly, *Escherichia coli* S17-1 λpir, carrying pMo130-TelR (*sacB*$^+$, *xylE*$^+$; Addgene, Watertown, MA, USA) embedded with an appropriate DNA fragment, was obtained by performing PCR with the primers listed in Table S2, after which the strain was conjugated with *A. baumannii* NU-60 on membrane filters placed on LB-agar plates and incubated for 24 h at 30°C. The membrane filter was washed with LB broth, and aliquots were placed on LB-agar plates containing chloramphenicol (30 μg/ml) and tellurite (30 μg/ml) for selecting *A. baumannii* conjugants featuring the first crossover replacement. Insertion of fragments derived from pMo130-TelR (*sacB*$^+$, *xylE*$^+$) was confirmed by spraying 0.45 M pyrocatechol as an indicator (pyrocatechol is converted to yellow-colored 2-hydroxymuconic semialdehyde by XylE). The conjugants featuring the first crossover replacement were passaged daily with LB broth containing 10% sucrose in order to select bacterial cells featuring a second crossover, which then resulted in the deletion of the targeted gene. Bacterial cells subsequently were grown on agar plates containing 10% sucrose, and the colonies that appeared were sprayed with 0.45 M pyrocatechol solution to confirm the loss of vector-derived fragments. The expected deletion of target genes was confirmed by performing PCR and sequencing analyses.

The *A. baumannii* ATCC 17978 strain, with *recA* gene replacement (*A. baumannii* ATCC 17978Δ*recA* strain), was constructed according to the previous method (64). The upstream and downstream regions of *recA* were separately amplified using the primers shown in Table S2. The *tet*(B) gene of *A. baumannii* strain NU-60 was also amplified. Overlap PCR was performed with the above-described three PCR products to obtain *tet*(B) gene cassettes flanked by *recA* upper and lower genetic regions. The constructed *tet*(B) gene cassettes were electroporated into *A. baumannii* ATCC 17978. The transformants

were selected on LB agar plates containing tetracycline. The designed gene replacement was confirmed by performing PCR and sequencing analyses. Complementation experiments were performed by introducing pKT230 plasmids carrying *recA* into the *A. baumannii* ATCC 17978Δ*recA* strain.

qPCR. qPCR analyses to estimate the copy numbers of *armA*, bla_{TEM-1}, and capsid 1 and 2 genes in purified DNA samples were performed using TB green premix EX *Taq* (TaKaRa) and a StepOnePlus system (Thermo Fisher Scientific). The primers used for qPCR are listed in Table S2; 0.4 ng of DNA was added to each reaction mixture, and qPCR was performed in a final volume of 20 μl.

Data availability. The complete genome sequence of *A. baumannii* strain NU-60 was deposited in GenBank under accession no. AP019685.

SUPPLEMENTAL MATERIAL

Supplemental material for this article may be found at https://doi.org/10.1128/AAC.00334-19.

SUPPLEMENTAL FILE 1, PDF file, 6.06 MB.

ACKNOWLEDGMENTS

This study was supported by grants from the JSPS KAKENHI (grant number JP26670211), the Hori Sciences and Arts Foundation, and the Waksman Foundation of Japan. We are grateful to Kouji Itakura (Division for Medical Research Engineering, Nagoya University Graduate School of Medicine) for technical support with TEM studies and Aiko Fujita (Nagoya University Graduate School of Medicine) for assistance.

REFERENCES

1. Harding CM, Hennon SW, Feldman MF. 2017. Uncovering the mechanisms of *Acinetobacter baumannii* virulence. Nat Rev Microbiol 16:91–102. https://doi.org/10.1038/nrmicro.2017.148.
2. McConnell MJ, Actis L, Pachon J. 2013. *Acinetobacter baumannii*: human infections, factors contributing to pathogenesis and animal models. FEMS Microbiol Rev 37:130–155. https://doi.org/10.1111/j.1574-6976.2012.00344.x.
3. Perez F, Hujer AM, Hujer KM, Decker BK, Rather PN, Bonomo RA. 2007. Global challenge of multidrug-resistant *Acinetobacter baumannii*. Antimicrob Agents Chemother 51:3471–3484. https://doi.org/10.1128/AAC.01464-06.
4. Matsui M, Suzuki M, Suzuki M, Yatsuyanagi J, Watahiki M, Hiraki Y, Kawano F, Tsutsui A, Shibayama K, Suzuki S. 2018. Distribution and molecular characterization of *Acinetobacter baumannii* international clone II lineage in Japan. Antimicrob Agents Chemother 62:e02190-17. https://doi.org/10.1128/AAC.02190-17.
5. Karah N, Sundsfjord A, Towner K, Samuelsen O. 2012. Insights into the global molecular epidemiology of carbapenem non-susceptible clones of *Acinetobacter baumannii*. Drug Resist Updat 15:237–247. https://doi.org/10.1016/j.drup.2012.06.001.
6. Pournaras S, Dafopoulou K, Del Franco M, Zarkotou O, Dimitroulia E, Protonotariou E, Poulou A, Zarrilli R, Tsakris A, Skoura L, Themeli-Digalaki K, Perivolioti E, Tsiplakou S, Karavassilis V, Panopoulou M, Orfanidou M, Hadjichristodoulou C, Levidiotou S, Gikas A, Greek Study Group on Acinetobacter Antimicrobial Resistance. 2017. Predominance of international clone 2 OXA-23-producing-*Acinetobacter baumannii* clinical isolates in Greece, 2015: results of a nationwide study. Int J Antimicrob Agents 49:749–753. https://doi.org/10.1016/j.ijantimicag.2017.01.028.
7. Mugnier PD, Poirel L, Naas T, Nordmann P. 2009. Worldwide dissemination of the bla_{OXA-23} carbapenemase gene of *Acinetobacter baumannii*. Emerg Infect Dis 16:35–40. https://doi.org/10.3201/eid1601.090852.
8. Wachino J, Arakawa Y. 2012. Exogenously acquired 16S rRNA methyltransferases found in aminoglycoside-resistant pathogenic Gram-negative bacteria: an update. Drug Resist Updat 15:133–148. https://doi.org/10.1016/j.drup.2012.05.001.
9. Yamane K, Wachino J-I, Doi Y, Kurokawa H, Arakawa Y. 2005. Global spread of multiple aminoglycoside resistance genes. Emerg Infect Dis 11:951–953. https://doi.org/10.3201/eid1106.040924.
10. Jones LS, Carvalho MJ, Toleman MA, White PL, Connor TR, Mushtaq A, Weeks JL, Kumarasamy KK, Raven KE, Torok ME, Peacock SJ, Howe RA, Walsh TR. 2015. Characterization of plasmids in extensively drug-resistant acinetobacter strains isolated in India and Pakistan. Antimicrob Agents Chemother 59:923–929. https://doi.org/10.1128/AAC.03242-14.
11. Blackwell GA, Holt KE, Bentley SD, Hsu LY, Hall RM. 2017. Variants of AbGRI3 carrying the *armA* gene in extensively antibiotic-resistant *Acinetobacter baumannii* from Singapore. J Antimicrob Chemother 72:1031–1039. https://doi.org/10.1093/jac/dkw542.
12. Hamidian M, Venepally P, Hall RM, Adams MD. 2017. Corrected genome sequence of *Acinetobacter baumannii* strain AB0057, an antibiotic-resistant isolate from lineage 1 of global clone 1. Genome Announc 5:e00836-17. https://doi.org/10.1128/genomeA.00836-17.
13. Shrestha S, Tada T, Miyoshi-Akiyama T, Ohara H, Shimada K, Satou K, Teruya K, Nakano K, Shiroma A, Sherchand JB, Rijal BP, Hirano T, Kirikae T, Pokhrel BM. 2015. Molecular epidemiology of multidrug-resistant *Acinetobacter baumannii* isolates in a university hospital in Nepal reveals the emergence of a novel epidemic clonal lineage. Int J Antimicrob Agents 46:526–531. https://doi.org/10.1016/j.ijantimicag.2015.07.012.
14. Krahn T, Wibberg D, Maus I, Winkler A, Bontron S, Sczyrba A, Nordmann P, Puhler A, Poirel L, Schluter A. 2016. Intraspecies transfer of the chromosomal *Acinetobacter baumannii* bla_{NDM-1} carbapenemase gene. Antimicrob Agents Chemother 60:3032–3040. https://doi.org/10.1128/AAC.00124-16.
15. Harding CM, Tracy EN, Carruthers MD, Rather PN, Actis LA, Munson RS, Jr. 2013. *Acinetobacter baumannii* strain M2 produces type IV pili which play a role in natural transformation and twitching motility but not surface-associated motility. mBio 4:e00360-13. https://doi.org/10.1128/mBio.00360-13.
16. Overballe-Petersen S, Harms K, Orlando LA, Mayar JV, Rasmussen S, Dahl TW, Rosing MT, Poole AM, Sicheritz-Ponten T, Brunak S, Inselmann S, de Vries J, Wackernagel W, Pybus OG, Nielsen R, Johnsen PJ, Nielsen KM, Willerslev E. 2013. Bacterial natural transformation by highly fragmented and damaged DNA. Proc Natl Acad Sci U S A 110:19860–19865. https://doi.org/10.1073/pnas.1315278110.
17. Wilharm G, Piesker J, Laue M, Skiebe E. 2013. DNA uptake by the nosocomial pathogen *Acinetobacter baumannii* occurs during movement along wet surfaces. J Bacteriol 195:4146–4153. https://doi.org/10.1128/JB.00754-13.
18. Biller SJ, McDaniel LD, Breitbart M, Rogers E, Paul JH, Chisholm SW. 2017. Membrane vesicles in sea water: heterogeneous DNA content and implications for viral abundance estimates. ISME J 11:394–404. https://doi.org/10.1038/ismej.2016.134.
19. Perez-Cruz C, Carrion O, Delgado L, Martinez G, Lopez-Iglesias C, Mercade E. 2013. New type of outer membrane vesicle produced by the Gram-negative bacterium *Shewanella vesiculosa* M7T: implications for DNA content. Appl Environ Microbiol 79:1874–1881. https://doi.org/10.1128/AEM.03657-12.
20. Dorward DW, Garon CF, Judd RC. 1989. Export and intercellular transfer

of DNA via membrane blebs of *Neisseria gonorrhoeae*. J Bacteriol 171: 2499–2505. https://doi.org/10.1128/jb.171.5.2499-2505.1989.
21. Fulsundar S, Harms K, Flaten GE, Johnsen PJ, Chopade BA, Nielsen KM. 2014. Gene transfer potential of outer membrane vesicles of *Acinetobacter baylyi* and effects of stress on vesiculation. Appl Environ Microbiol 80:3469–3483. https://doi.org/10.1128/AEM.04248-13.
22. Rumbo C, Fernandez-Moreira E, Merino M, Poza M, Mendez JA, Soares NC, Mosquera A, Chaves F, Bou G. 2011. Horizontal transfer of the OXA-24 carbapenemase gene via outer membrane vesicles: a new mechanism of dissemination of carbapenem resistance genes in *Acinetobacter baumannii*. Antimicrob Agents Chemother 55:3084–3090. https://doi.org/10.1128/AAC.00929-10.
23. Chatterjee S, Mondal A, Mitra S, Basu S. 2017. *Acinetobacter baumannii* transfers the bla_{NDM-1} gene via outer membrane vesicles. J Antimicrob Chemother 72:2201–2207. https://doi.org/10.1093/jac/dkx131.
24. Jurcisek JA, Brockman KL, Novotny LA, Goodman SD, Bakaletz LO. 2017. Nontypeable *Haemophilus influenzae* releases DNA and DNABII proteins via a T4SS-like complex and ComE of the type IV pilus machinery. Proc Natl Acad Sci U S A 114:E6632–E6641. https://doi.org/10.1073/pnas.1705508114.
25. Hamilton HL, Dominguez NM, Schwartz KJ, Hackett KT, Dillard JP. 2005. *Neisseria gonorrhoeae* secretes chromosomal DNA via a novel type IV secretion system. Mol Microbiol 55:1704–1721. https://doi.org/10.1111/j.1365-2958.2005.04521.x.
26. Wallden K, Rivera-Calzada A, Waksman G. 2010. Type IV secretion systems: versatility and diversity in function. Cell Microbiol 12: 1203–1212. https://doi.org/10.1111/j.1462-5822.2010.01499.x.
27. Croucher NJ, Mostowy R, Wymant C, Turner P, Bentley SD, Fraser C. 2016. Horizontal DNA transfer mechanisms of bacteria as weapons of intragenomic conflict. PLoS Biol 14:e1002394. https://doi.org/10.1371/journal.pbio.1002394.
28. Lang AS, Westbye AB, Beatty JT. 2017. The distribution, evolution, and roles of gene transfer agents in prokaryotic genetic exchange. Annu Rev Virol 4:87–104. https://doi.org/10.1146/annurev-virology-101416-041624.
29. Lang AS, Zhaxybayeva O, Beatty JT. 2012. Gene transfer agents: phage-like elements of genetic exchange. Nat Rev Microbiol 10:472–482. https://doi.org/10.1038/nrmicro2802.
30. McDaniel LD, Young E, Delaney J, Ruhnau F, Ritchie KB, Paul JH. 2010. High frequency of horizontal gene transfer in the oceans. Science 330: 50. https://doi.org/10.1126/science.1192243.
31. Vaneechoutte M, Young DM, Ornston LN, De Baere T, Nemec A, Van Der Reijden T, Carr E, Tjernberg I, Dijkshoorn L. 2006. Naturally transformable *Acinetobacter* sp. strain ADP1 belongs to the newly described species *Acinetobacter baylyi*. Appl Environ Microbiol 72:932–936. https://doi.org/10.1128/AEM.72.1.932-936.2006.
32. Yildirim S, Thompson MG, Jacobs AC, Zurawski DV, Kirkup BC. 2016. Evaluation of parameters for high efficiency transformation of *Acinetobacter baumannii*. Sci Rep 6:22110. https://doi.org/10.1038/srep22110.
33. Du XD, Li DX, Hu GZ, Wang Y, Shang YH, Wu CM, Liu HB, Li XS. 2012. Tn*1548*-associated *armA* is co-located with *qnrB2*, *aac(6')-Ib-cr* and $bla_{CTX-M-3}$ on an IncFII plasmid in a *Salmonella enterica* subsp. *enterica serovar* Paratyphi B strain isolated from chickens in China. J Antimicrob Chemother 67:246–248. https://doi.org/10.1093/jac/dkr407.
34. Galimand M, Sabtcheva S, Courvalin P, Lambert T. 2005. Worldwide disseminated armA aminoglycoside resistance methylase gene is borne by composite transposon Tn*1548*. Antimicrob Agents Chemother 49: 2949–2953. https://doi.org/10.1128/AAC.49.7.2949-2953.2005.
35. Tada T, Miyoshi-Akiyama T, Shimada K, Nga TTT, Thu LTA, Son NT, Ohmagari N, Kirikae T. 2015. Dissemination of clonal complex 2 *Acinetobacter baumannii* strains co-producing carbapenemases and 16S rRNA methylase ArmA in Vietnam. BMC Infect Dis 15:433. https://doi.org/10.1186/s12879-015-1171-x.
36. Zhou H, Zhang TW, Yu DL, Pi BR, Yang Q, Zhou JY, Hu SN, Yu YS. 2011. Genomic analysis of the multidrug-resistant *Acinetobacter baumannii* strain MDR-ZJ06 widely spread in China. Antimicrob Agents Chemother 55:4506–4512. https://doi.org/10.1128/AAC.01134-10.
37. Schwechheimer C, Kuehn MJ. 2015. Outer-membrane vesicles from Gram-negative bacteria: biogenesis and functions. Nat Rev Microbiol 13:605–619. https://doi.org/10.1038/nrmicro3525.
38. Jin JS, Kwon SO, Moon DC, Gurung M, Lee JH, Kim SI, Lee JC. 2011. *Acinetobacter baumannii* secretes cytotoxic outer membrane protein A via outer membrane vesicles. PLoS One 6:e17027. https://doi.org/10.1371/journal.pone.0017027.
39. McConnell MJ, Rumbo C, Bou G, Pachon J. 2011. Outer membrane vesicles as an acellular vaccine against *Acinetobacter baumannii*. Vaccine 29:5705–5710. https://doi.org/10.1016/j.vaccine.2011.06.001.
40. Daleke-Schermerhorn MH, Felix T, Soprova Z, ten Hagen-Jongman CM, Vikström D, Majlessi L, Beskers J, Follmann F, de Punder K, van der Wel NN, Baumgarten T, Pham TV, Piersma SR, Jiménez CR, van Ulsen P, de Gier J-W, Leclerc C, Jong WSP, Luirink J. 2014. Decoration of outer membrane vesicles with multiple antigens by using an autotransporter approach. Appl Environ Microbiol 80:5854–5865. https://doi.org/10.1128/AEM.01941-14.
41. Perez-Cruz C, Delgado L, Lopez-Iglesias C, Mercade E. 2015. Outer-inner membrane vesicles naturally secreted by gram-negative pathogenic bacteria. PLoS One 10:e0116896. https://doi.org/10.1371/journal.pone.0116896.
42. Carruthers MD, Nicholson PA, Tracy EN, Munson RS. 2013. *Acinetobacter baumannii* utilizes a type VI secretion system for bacterial competition. PLoS One 8:e59388. https://doi.org/10.1371/journal.pone.0059388.
43. Hood RD, Singh P, Hsu FS, Guvener T, Carl MA, Trinidad RRS, Silverman JM, Ohlson BB, Hicks KG, Plemel RL, Li M, Schwarz S, Wang WY, Merz AJ, Goodlett DR, Mougous JD. 2010. A type VI secretion system of *Pseudomonas aeruginosa* targets, a toxin to bacteria. Cell Host Microbe 7:25–37. https://doi.org/10.1016/j.chom.2009.12.007.
44. Stanczak-Mrozek KI, Laing KG, Lindsay JA. 2017. Resistance gene transfer: induction of transducing phage by sub-inhibitory concentrations of antimicrobials is not correlated to induction of lytic phage. J Antimicrob Chemother 72:1624–1631. https://doi.org/10.1093/jac/dkx056.
45. Fujisawa H, Morita M. 2003. Phage DNA packaging. Genes Cells 2:537–545. https://doi.org/10.1046/j.1365-2443.1997.1450343.x.
46. Quiros P, Colomer-Lluch M, Martinez-Castillo A, Miro E, Argente M, Jofre J, Navarro F, Muniesa M. 2014. Antibiotic resistance genes in the bacteriophage DNA fraction of human fecal samples. Antimicrob Agents Chemother 58:606–609. https://doi.org/10.1128/AAC.01684-13.
47. Gunathilaka GU, Tahlan V, Ibn Mafiz A, Polur M, Zhang YF. 2017. Phages in urban wastewater have the potential to disseminate antibiotic resistance. Int J Antimicrobial Agents 50:678–683. https://doi.org/10.1016/j.ijantimicag.2017.08.013.
48. Marti E, Variatza E, Balcazar JL. 2014. Bacteriophages as a reservoir of extended-spectrum beta-lactamase and fluoroquinolone resistance genes in the environment. Clin Microbiol Infect 20:O456–O459. https://doi.org/10.1111/1469-0691.12446.
49. Balcazar JL. 2014. Bacteriophages as vehicles for antibiotic resistance genes in the environment. PLoS Pathog 10:e1004219. https://doi.org/10.1371/journal.ppat.1004219.
50. Tada T, Miyoshi-Akiyama T, Shimada K, Shimojima M, Kirikae T. 2014. Dissemination of 16S rRNA methylase ArmA-producing *Acinetobacter baumannii* and emergence of OXA-72 carbapenemase coproducers in Japan. Antimicrob Agents Chemother 58:2916–2920. https://doi.org/10.1128/AAC.01212-13.
51. Lee Y, D'Souza R, Yong D, Lee K. 2016. Prediction of putative resistance islands in a carbapenem-resistant *Acinetobacter baumannii* global clone 2 clinical isolate. Ann Lab Med 36:320–324. https://doi.org/10.3343/alm.2016.36.4.320.
52. Park JY, Kim S, Kim SM, Cha SH, Lim SK, Kim J. 2011. Complete genome sequence of multidrug-resistant *Acinetobacter baumannii* strain 1656-2, which forms sturdy biofilm. J Bacteriol 193:6393–6394. https://doi.org/10.1128/JB.06109-11.
53. Lean SS, Yeo CC, Suhaili Z, Thong KL. 2015. Comparative genomics of two ST 195 carbapenem-resistant *Acinetobacter baumannii* with different susceptibility to polymyxin revealed underlying resistance mechanism. Front Microbiol 6:1445. https://doi.org/10.3389/fmicb.2015.01445.
54. Holt KE, Hamidian M, Kenyon JJ, Wynn MT, Hawkey J, Pickard D, Hall RM. 2015. Genome sequence of *Acinetobacter baumannii* strain A1, an early example of antibiotic-resistant global clone 1. Genome Announc 3:e00032-15. https://doi.org/10.1128/genomeA.00032-15.
55. Koren S, Walenz BP, Berlin K, Miller JR, Bergman NH, Phillippy AM. 2017. Canu: scalable and accurate long-read assembly via adaptive k-mer weighting and repeat separation. Genome Res 27:722–736. https://doi.org/10.1101/gr.215087.116.
56. Walker BJ, Abeel T, Shea T, Priest M, Abouelliel A, Sakthikumar S, Cuomo CA, Zeng Q, Wortman J, Young SK, Earl AM. 2014. Pilon: an integrated tool for comprehensive microbial variant detection and genome assembly improvement. PLoS One 9:e112963. https://doi.org/10.1371/journal.pone.0112963.
57. Tanizawa Y, Fujisawa T, Nakamura Y. 2018. DFAST: a flexible prokaryotic

genome annotation pipeline for faster genome publication. Bioinformatics 34:1037–1039. https://doi.org/10.1093/bioinformatics/btx713.
58. Coil D, Jospin G, Darling AE. 2015. A5-miseq: an updated pipeline to assemble microbial genomes from Illumina MiSeq data. Bioinformatics 31:587–589. https://doi.org/10.1093/bioinformatics/btu661.
59. Zankari E, Hasman H, Cosentino S, Vestergaard M, Rasmussen S, Lund O, Aarestrup FM, Larsen MV. 2012. Identification of acquired antimicrobial resistance genes. J Antimicrob Chemother 67:2640–2644. https://doi.org/10.1093/jac/dks261.
60. Arndt D, Grant JR, Marcu A, Sajed T, Pon A, Liang Y, Wishart DS. 2016. PHASTER: a better, faster version of the PHAST phage search tool. Nucleic Acids Res 44:W16–W21. https://doi.org/10.1093/nar/gkw387.
61. Alikhan NF, Petty NK, Ben Zakour NL, Beatson SA. 2011. BLAST ring image generator (BRIG): simple prokaryote genome comparisons. BMC Genomics 12:402. https://doi.org/10.1186/1471-2164-12-402.
62. Clinical and Laboratory Standards Institute. 2014. Performance standards for antimicrobial susceptibility testing: twenty-fourth informational supplement, M100-S24. CLSI, Wayne, PA.
63. Amin IM, Richmond GE, Sen P, Koh TH, Piddock LJ, Chua KL. 2013. A method for generating marker-less gene deletions in multidrug-resistant *Acinetobacter baumannii*. BMC Microbiol 13:158. https://doi.org/10.1186/1471-2180-13-158.
64. Aranda J, Poza M, Pardo BG, Rumbo S, Rumbo C, Parreira JR, Rodriguez-Velo P, Bou G. 2010. A rapid and simple method for constructing stable mutants of *Acinetobacter baumannii*. BMC Microbiol 10:279. https://doi.org/10.1186/1471-2180-10-279.